TECHNICAL MEMORANDUM

490

Wind-Driven Eddies and Plankton Blooms in the North Atlantic Ocean

C. Eden[1] and T. Jung

Research Department

[1] IFM-GEOMAR, Kiel, Germany

Submitted to J. Climate.

March 2006

European Centre for Medium-Range Weather Forecasts
Europäisches Zentrum für mittelfristige Wettervorhersage
Centre européen pour les prévisions météorologiques à moyen terme

Series: ECMWF Technical Memoranda

A full list of ECMWF Publications can be found on our web site under:
http://www.ecmwf.int/publications/

Contact: library@ecmwf.int

Abstract

Recent high-resolution satellite missions have revealed persistent small-scale features in near surface winds over the global oceans (Liu et al., 2000; Xie et al., 2001; Chelton et al., 2004). Here we report that such features — in contrast to previous belief (Chelton et al., 2004) — also show up in numerical weather prediction models such as the operational high-resolution model of the European Centre for Medium-Range Weather Forecasts (ECMWF). We exploit this finding by forcing a high-resolution general circulation model of the North Atlantic ocean over a 4-year period with surface wind stress and heat fluxes taken from the ECMWF model. Driven by the orographically forced small-scales features in the wind forcing, in our simulation, meso-scale oceanic eddies develop in the lee of Islands located in areas of prevailing trade winds such as the Cape Verde Islands. These eddies can provide a substantial, previously overlooked source of oceanic eddy kinetic energy in subtropical regions. Furthermore, anticlockwise circulating eddies are related to upwelling of nutrient rich water from below leading to large plankton blooms in the simulations. It is speculated that similar eddies also show up at comparable other locations in the world oceans, e.g. the Hawaiian Archipelago, with far-reaching implications for local and basin-wide ecosystem dynamics.

1 Introduction

The stress of the wind over the surface of the ocean causes currents, which can be of the same order of magnitude as tidal currents, or sometimes even stronger. While tidal currents are almost neglectible when averaged over tidal periods, wind-driven currents show a significant non-vanishing mean. In fact, the mean wind forcing is responsible for the most energetic large-scale, near surface current systems such as the Kurushio in the North Pacific Ocean or the Equatorial Undercurrent in each of the tropical oceans. Seasonal varying winds can also force seasonal currents, such as in the Indian Ocean, where strong reversing currents of similar amplitude as the steady ones are generated in response to the seasonally changing Indian summer monsoon circulation (Schott and McCreary, 2001). On the other hand, much of the energy of the oceanic circulation is contained in fluctuating kinetic and potential energy signals of turbulent nature (Wunsch and Ferrari, 2004). This is because the mean or seasonally varying wind forcing generates a large pool of mean kinetic and potential energy, on which perturbations can grow exponentially due to hydrodynamically unstable mean states, feeding meso-scale turbulence in the ocean. This turbulent motion represents what is commonly called "eddies" amongst oceanographers and takes place on space and time scales of the order of 10–100 *km* and 10–100 *days*, respectively (Stammer and Böning, 1996).

It has been speculated in the past that part of the energy contained in the eddy-field of the ocean might be directly driven by synoptic-scale wind fluctuations associated with the passage of atmospheric low pressure systems, and not indirectly by the hydrodynamical instabilities (Frankignoul and Müller, 1979; Müller and Frankignoul, 1981). However, it is hard to see how the synoptic-scale atmospheric weather systems on much larger spatial ($>$1000 *km*) and shorter temporal scale (2–7 *days*) can generate oceanic eddies. In fact, recent ocean general circulation model (OGCM) studies (Stammer et al., 2001) suggest that the impact on eddies by synoptic-scale windstress forcing is rather low and contributes only a few percent to the total energy stored in oceanic eddies. Here we show, using high-resolution models of both the atmosphere and ocean, how realistic small-scale, persistent sub-synoptic features of the wind stress forcing in the ECMWF model, which have been absent from the relatively low-resolution forcing used in previous ocean modeling studies, provide a significant source of eddy variability in the ocean.

With increasing temporal and spatial resolution achieved by recent satellite missions it is now possible to obtain a more detailed and realistic estimate of the wind stress forcing of the ocean than ever before. In fact, many persistent small-scale features have been reported from satellite data which were previously unknown due to the sparseness of the observations (Liu et al., 2000; Xie et al., 2001; Chelton et al., 2004). However, the use of satellite-based observations to force OGCMs is still problematic, due to gaps in the time series and missing consistent information for complementary forcing products such as surface heat and freshwater fluxes. Numerical weather prediction (NWP) models, on the other hand, do provide all surface forcing functions in a dynamically consistent way. This fact has been extensively exploited by the climate research community through the use of decadal-scale long NWP model-based reanalysis products (Kalnay et al., 1996; Uppala et al., 2006). These datasets, however, suffer from relatively low spatial resolution compared to NWP models used operationally to carry out weather forecasts. Here we use one of the most advanced NWP models available, the ECMWF model, to construct high-resolution, dynamically consistent surface forcing fields for driving a state-of-the-art high-resolution OGCM. To our knowledge these forcings fields have the highest spatial resolution and the most realistic small-scale characteristics (Janssen, 2004) used so far to consistently drive OGCMs.

In the next section, the OGCM and the forcing functions will be presented, followed in section 3 by a discussion of the small-scale features in near surface winds showing up both in the ECMWF model and in recent high-resolution satellite observations. In section 4 the oceanic response to such features is presented, mechanism and effects are explored using sensitivity experiments with the OGCM. In section 5 the response of a biogeochemical model coupled to the OGCM is analyzed and the last section summarizes and discussses the results.

2 Models

The ECMWF model is a global spectral model (T_L511) with horizontal resolution of about $40 \times 40\,km$ and 60 vertical levels. It consists of a dynamical component, a physical component and a coupled ocean wave component[1]. A four-dimensional variational data assimilation scheme is used for producing the analysis (Rabier et al., 2000; Mahfouf and Rabier, 2000). Daily forcing fields were obtained from 24-hour forecasts started from operational analyses at 12 Universal Coordinated Time (UTC) of each of the days for the years 2001 to 2004.

The OGCM is a grid-point model with horizontal resolution of about $10\,km$ at the equator increasing to about $5\,km$ at 70^oN and 45 vertical levels, ranging from $10\,m$ at the surface to $250\,m$ near the maximal depth of $5500\,m$. The model domain extents from 20^oS to 70^oN with open boundaries at the northern and southern boundaries and with a restoring zone in the eastern Mediterranean Sea. The model is based on a rewritten version[2] of MOM2 (Pacanowski, 1995) and is identical to the one used in Dengler et al. (2004) except for the surface forcing. It was integrated for 10 years in a spinup phase with monthly climatological forcing (Barnier et al., 1995), after which the daily forcing in wind stress, heat fluxes and friction velocity taken from the ECMWF model was applied for the years 2001 to 2004. Note that the friction velocity parameterizes the wind input of small-scale oceanic turbulence affecting the mixed layer turbulence closure model (Gaspar et al., 1990) only. Note also that the monthly mean climatological forcing was derived from an earlier, coarser resolution (about $200\,km$) version of the ECMWF model (operationally used during the years 1986–1990) as a common dataset in the European "DYNAMO" ocean model intercomparison project (Willebrand et al., 2001) and was used extensively in many model studies since then (e.g. Eden and Jung, 2001).

The OGCM was integrated, after the 10 year spinup phase, for additional 20 years with the climatological forcing coupled to a nitrate-based, four compartment ecosystem model. The biogeochemical model is identical to the one in Oschlies and Garçon (1998) and Eden and Oschlies (2006). After the 10-year spinup phase the high resolution forcing of wind stress, heat flux and friction velocity taken from the ECMWF NWP model for the years 2001 to 2004 was again applied to drive the coupled physical-biogeochemical model.

[1] Further information is available at *http://www.ecmwf.int*

[2] The numerical code together with all configurations used in this study can be accessed at *http://www.ifm.uni-kiel.de/fb/fb1/tm/data/pers/ceden/spflame/index.html*.

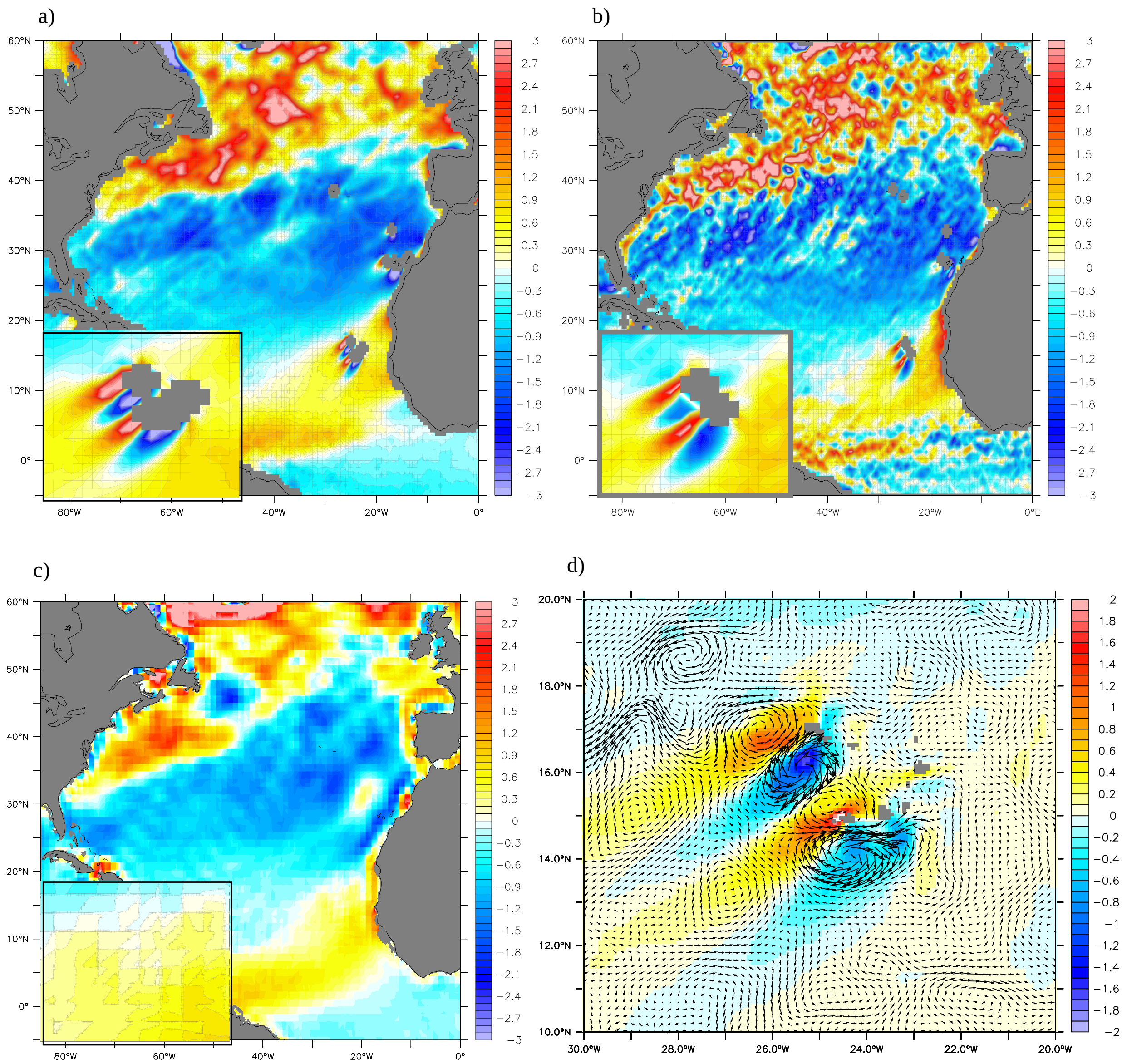

Figure 1: Wind stress curl in $N/m^3 \times 10^7$ averaged from 1 January to 15 May 2001 from the ECMWF model (a), satellite scatterometer derived windstress from QuikSCAT (b) and climatological wind stress curl, which is used to drive the ocean model in a spinup phase averaged for the same season (c). Also shown in the lower left corner of figures a–c is a more detailed view of the wind stress curl in the region around the Cape Verde Islands. d) Wind stress curl in $N/m^3 \times 10^6$ on 21 April 2001 (shaded) and velocity at 50m depth in the region around the Cape Verde Islands (arrows). Arrows are shown at every second gridpoint. The maximum arrow length corresponds to about 0.5 m/s.

3 Small-scale wind stress features

The mean wintertime wind stress curl (curl $\tau = k \times \nabla_h \tau$, where τ denotes the wind stress vector) averaged from 1 January to 15 May 2001 over the North Atlantic is shown in Fig. 1 for the ECMWF model (Fig. 1 a) and satellite observations (Fig. 1 b) taken from QuikSCAT[3]. Also shown in the lower left corner of the figures is a more detailed view of the wind stress curl in the region around the Cape Verde Islands. Note that we show the wind stress curl because the wind stress divergence plays a negligible role in generating ocean currents, since ageostrophic motion, that is, the dynamically important part of the flow deviating from the dominating balance between the pressure and the Coriolis forces, is given by conservation of angular momentum and, therefore, driven by curl τ (Gill, 1982). Note also that no QuikSCAT data were assimilated at ECMWF in 2001 allowing to use QuikSCAT data for model evaluation.

As expected the large scale pattern of curl τ in the ECMWF model is very similar to the observational estimates. On the other hand, many small-scale structures evident in the high resolution satellite data are also present in the ECMWF model. In fact, it appears that there are more (and finer) small-scale structures showing up in the ECMWF model than in the observations, maybe due to strong spatial smoothing during processing of the satellite data. The realism of the ECMWF model in simulating such small-scale surface wind features is particular striking in the vicinity of the Cape Verde Islands, a group of islands in the North Atlantic west of Senegal. A band of banners of alternating curl τ shows up in lee of the archipelago both in the ECMWF model and the satellite observations; two positive and two negative banners extending about 400 km south-westward into the North Atlantic. This band is generated by the disturbance of the trade winds by the Islands (Schaer and Durran, 1997), which penerate more than 2 km into the troposphere. The obstacles induce upstream blocking which forces the flow to split leading to weaker winds behind them and stronger winds at the flanks of the quieter wind zone. Similar persistent small-scale patterns of curl τ show up at the Canary Islands and Madeira and at similar subtropical Islands around the globe.

In contrast, the small-scale features described above are completely missing in typical wind stress products used previously to force high-resolution OGCMs. This can be seen from Fig. 1 c), which shows the climatological wintertime curl τ driving the OGCM in the standard setup of the model and also in the spinup phase preceeding the integration discussed above. Note that the climatological wind stress forcing was derived from an earlier, coarse resolution (about 150 km) ECMWF model version. Thus, the small-scale wind stress features are missing in Fig. 1 c) most likely due to the coarse resolution used in older version of the ECMWF model. Furthermore, is is likely that most of the small-scale features such as the elongated bands of curl τ along the continental margins are artifacts due to the spectral truncation of surface topography in the low-resolution spectral NWP model from which the forcing was derived (Chelton et al., 2004).

4 Oceanic response

In the OGCM the ocean currents rapidly adjust to the small-scale atmospheric forcing. For instance, inside the four curl τ banners in the wind wake of the Cape Verde Islands, two cyclonic eddies related to positive curl τ and two anticyclonic eddies related to the negative banners of curl τ are frequently developing. Fig. 1 d) shows a typical situation in April 2001 while Fig. 2 shows a sequence of figures similar to Fig. 1 d) starting in 15. January of the following year 2002 and ending at 4. April 2002. The wind stress evidently generates coherent eddies with swirl velocities of up to 1 m/s. Such strong geostrophic eddies represent a very energetic flow for open ocean conditions; instantaneous velocities in the Gulf Stream and the Equatorial Undercurrents, for instance, rarely exceed 1 m/s and swirl velocities for open-ocean, whereas coherent eddies generated by hydrodynamic instabilities amount typically to no more than 10 cm/s.

Similar coherent oceanic eddies develop in the lee of the Canary Islands and Madeira, although they tend to

[3] The QuikSCAT satellite carries a specialized radar that measures near-surface wind speed and direction at 25 km resolution twice per day. The gridded vector wind stress τ from QuikSCAT has been obtained at Centre ERS d'Archivage et de Traitement (CERSAT), at IFREMER, Plouzane, France.

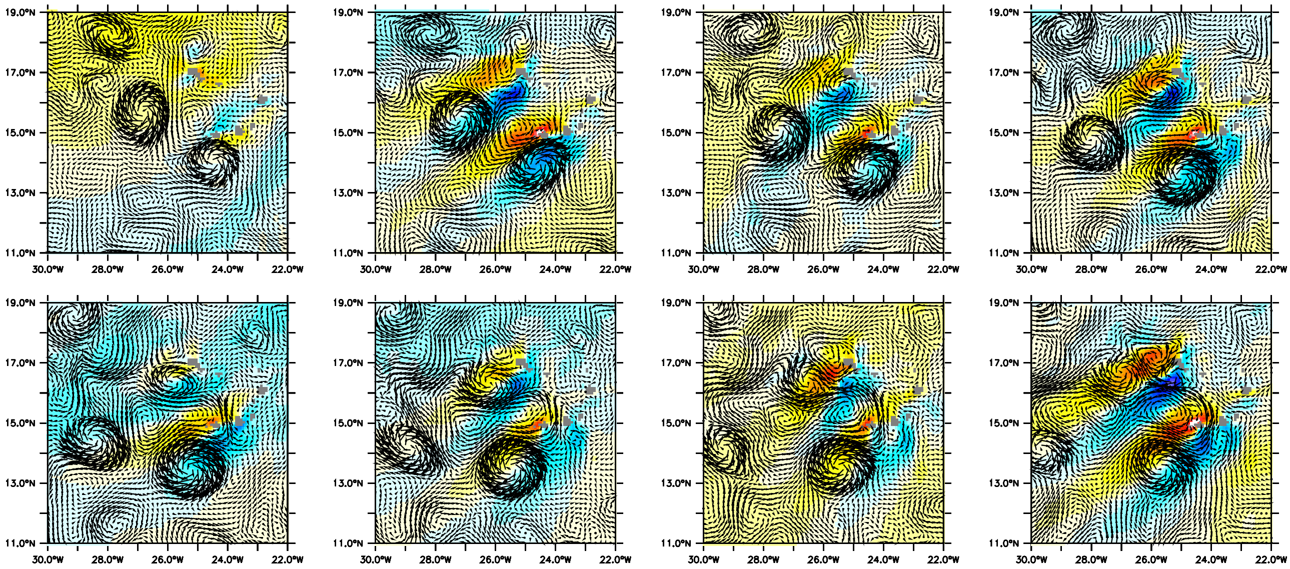

Figure 2: Sequence of velocity (arrows) in 50m depth near the Cape Verde Islands and wind stress curl (shaded in $N/m^3 \times 10^7$, color coding is the same as in Fig. 1) starting in the upper left panel on 15 January 2002 and ending in the lower right panel in 12 days steps.

be weaker and more infrequent during wintertime. In boreal summer, however, when the trade winds migrate northwards, Madeira and the Canary Islands represent much larger sources of oceanic eddies (not shown). In general, the anticyclonic eddies tend to be stronger than the cyclonic eddies, most likely since cyclones are related to upwelling, that is. colder surface water, which is rapidly heated by the atmosphere, while anticyclonic eddies show up as warmer surface water with, however, much weaker magnitudes. An interesting feature is also that the eddies leave the vicinity of the Cape Verde Islands and begin to propagate westwards once the forcing weakens as seen for instance in Fig. 2.

Simulated time series of wind stress amplitude, curl τ and relative vorticity (ζ) at 50m depth south-west of the Cape Verdes inside the four curl τ banners of the mean forcing (see Fig. 1) are shown in Fig. 3. $\zeta = k \times \nabla_h u_h$ is the curl of the horizontal flow u_h in the ocean and is directly forced by curl τ. Negative (positive) ζ denotes anticyclonic (cyclonic) flow (anticyclonic flow circulates clockwise in the Northern Hemisphere). Clearly, there is a positive correlation between the wind stress amplitude (i.e., the strength of the trade winds) and curl τ. The correlation is most prominent for the annual cycle; the strenghtening of the north-easterly trade winds in winter, for example, is accompanied by a corresponding increase in curl τ. Since negative (positive) curl τ is forcing negative (positive) ζ, i.e. anticyclonic (cyclonic) eddies, curl τ and ζ tend to covary. Note that curl τ and ζ covary not only at seasonal but also on subseasonal time scales.

It is worth pointing out that these eddies do not show up in simulations with the same OGCM when low-resolution forcing wind stress forcing is used. To demonstrate this, two additional experiments are performed with the OGCM in addition to the experiment in which the model was driven by the realistic, high-resolution forcing taken from the ECMWF model (HIGH hereafter): The first experiment (HIGH-WIND) in which the model was forced with high-resolution forcing in wind stress only for the years 2001 - 2004 following the 10-year spinup period while heat flux and friction velocity and all other forcing functions stay climatological as in the spinup. The second auxilliary experiment (LOW-WIND) is identical to HIGH-WIND but the daily wind stress was taken from the National Centers for Environmental Prediction/National Center For Atmospheric Research (NCEP/NCAR) reanalysis (Kalnay et al., 1996). Note that the horizontal resolution of the NCEP model corresponds to about 200 km, which is even coarser than the forcing used during the spinup phase.

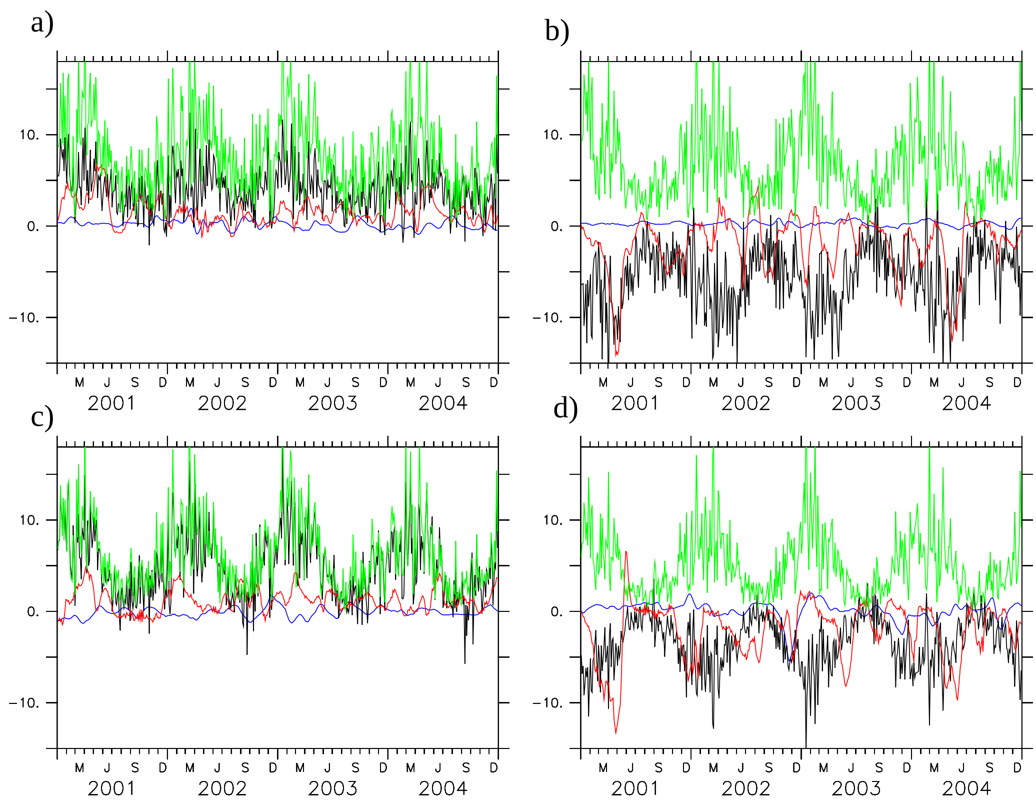

Figure 3: Time series of relative vorticity in the ocean model at 50m depth (red, in $s^{-1} \times 10^6$), wind stress curl (black, in $N/m^3 \times 10^7$) and wind stress amplitude (green, in $N/m^2 \times 100$) in lee of the Cape Verde Island at 17^oN, 26^oW (a), 16^oN,25.3^oW (b), 14.8^oN, 25^oW (c) and 14.2^oN, 24.2^oW (d). The blue line denotes relative vorticity in a simulation in which the model was forced with the coarse resolution forcing.

In experiment LOW-WIND, coherent eddies (as seen in Fig. 1 d) and Fig. 2) are absent, while they are present in experiment HIGH-WIND. The blue line in Fig. 3 shows relative vorticity ζ in lee of the Cape Verde Islands inside the four banners of wind stress curl anomalies in experiment LOW-WIND. Clearly, only weak eddy-signals are present in LOW-WIND at this location, compared to the strong relative vorticity which is generated in experiment HIGH (and HIGH-WIND, not shown). To further quantify the effect of the high-resolution forcing, Fig. 4 shows the results of the experiments in terms of near surface eddy kinetic energy (EKE) horizontally averaged over the south-eastern subtropical gyre. South of 30^oN EKE is increased by 20% to 60% in experiment HIGH and HIGH-WIND using the high-resolution wind forcing compared to the simulation with low-resolution forcing (LOW). Furthermore, it turns out that it is the daily wind stress forcing and not the daily heat flux forcing or friction velocity, which is responsible for the increased EKE in the simulation with the high-resolution forcing, since both experiments, HIGH and HIGH-WIND, show similar elevated levels of EKE.

Unfortunately, direct oceanographic observations, which could be used to compare the small-scale features found in the OGCM, are sparse[4]. An alternative source of observation we might rely upon are satellite altimeter datasets, which measure the sea surface elevation and, thus, geostrophic velocities. Fig. 5 shows EKE estimated from satellite altimeter observations[5] and from the experiments HIGH and LOW-WIND in the south-eastern

[4] For instance, only two surface drifters have been found in the World OCean Experiment (WOCE) database located in the vicinity of the Cape Verde Islands, one, in July apparently caught in a cyclonic eddy and one showing much weaker eddying motion in December (not shown).

[5] The altimeter products have been produced by SSALTO/DUACS and are distributed by AVISO.

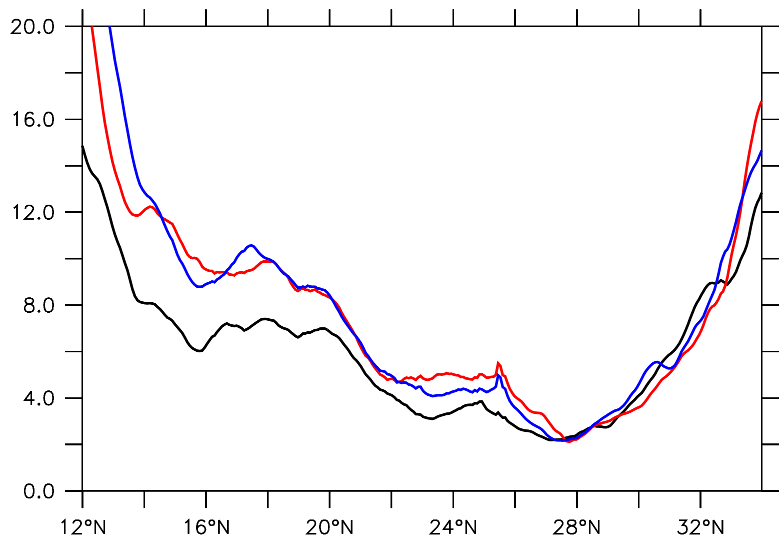

Figure 4: Eddy kinetic energy in cm^2/s^2 averaged between 50^oW and 15^oW in the model integration with high-resolution ECMWF forcing (exp. HIGH, red line) and high-resolution forcing in wind stress only (exp. HIGH-WIND, blue line) and an integration with daily wind stress forcing taken from the NCEP reanalysis (Kalnay et al., 1996) for the same time period (exp. LOW-WIND, black line).

subtropical gyre. It is evident from the figure, that the EKE calculated from altimeter data shows a local maximum in the vicinity of the Cape Verde Islands, consistent with our model results with high-resolution forcing (HIGH); this maximum, however, is absent if the low-resolution forcing is used (LOW-WIND). Note that the EKE in HIGH-WIND is almost identical to HIGH. Note also that the EKE estimated from the altimeter data appears to be significantly lower compared to the model results with high-resolution forcing in the vicinity of the Cape Verde. Such a bias does not only show up at this special location but also basin-wide in the model and is known to be a common bias for EKE derived from satellite altimeter data (Fratantoni, 2001). It should also be mentioned that altimeter observation can be obscured by incomplete removal of tidal currents near coastlines and shelf regions (Le Traon et al., 1995) as seen in the figure near the coast of Africa.

5 Ecosystem response

There is also a significant influence of the eddies generated by small-scale features of the wind stress on local ecosystem dynamics. Fig. 6 shows the biomass (vertically integrated in the upper water column) near the Cape Verde Island in spring 2001 in a simulation in which the OGCM (exp. HIGH) was coupled to a simple pelagic ecosystem model. As expected, there is high productivity and thus large biomass along the coastline of the African continent due to continuous wind-driven upwelling of nutrient-rich water. More surprisingly, however, another patch of high biomass is evident in lee of the Cape Verde Islands inbetween two anticyclonic eddies. The amplitude of the biomass patch in lee of the Cape Verde Islands is comparable to those found in the coastal upwelling region. Clearly, this patch is a result of the existence of the persistent small-scale cyclonic wind stress banners (see Fig. 1 a), which are related to upwelling of nutrient-rich water. Similar effects of the small-scale features in the wind stress curl show up near Madeira and the Canary Islands (not shown).

No such plankton blooms are found in simulations with low-resolution forcing: Fig. 7 shows a time series of near surface chlorophyll at a section along 15.5^oN in experiment HIGH (Fig. 7 a) and in the preceeding spinup integration with the lower-resolution atmospheric forcing (Fig. 7 b). We have used a factor of 1.59 $mg/mmol$ to convert the nitrate content of phytoplankton to an equivalent chlorophyll concentration. It is evident that

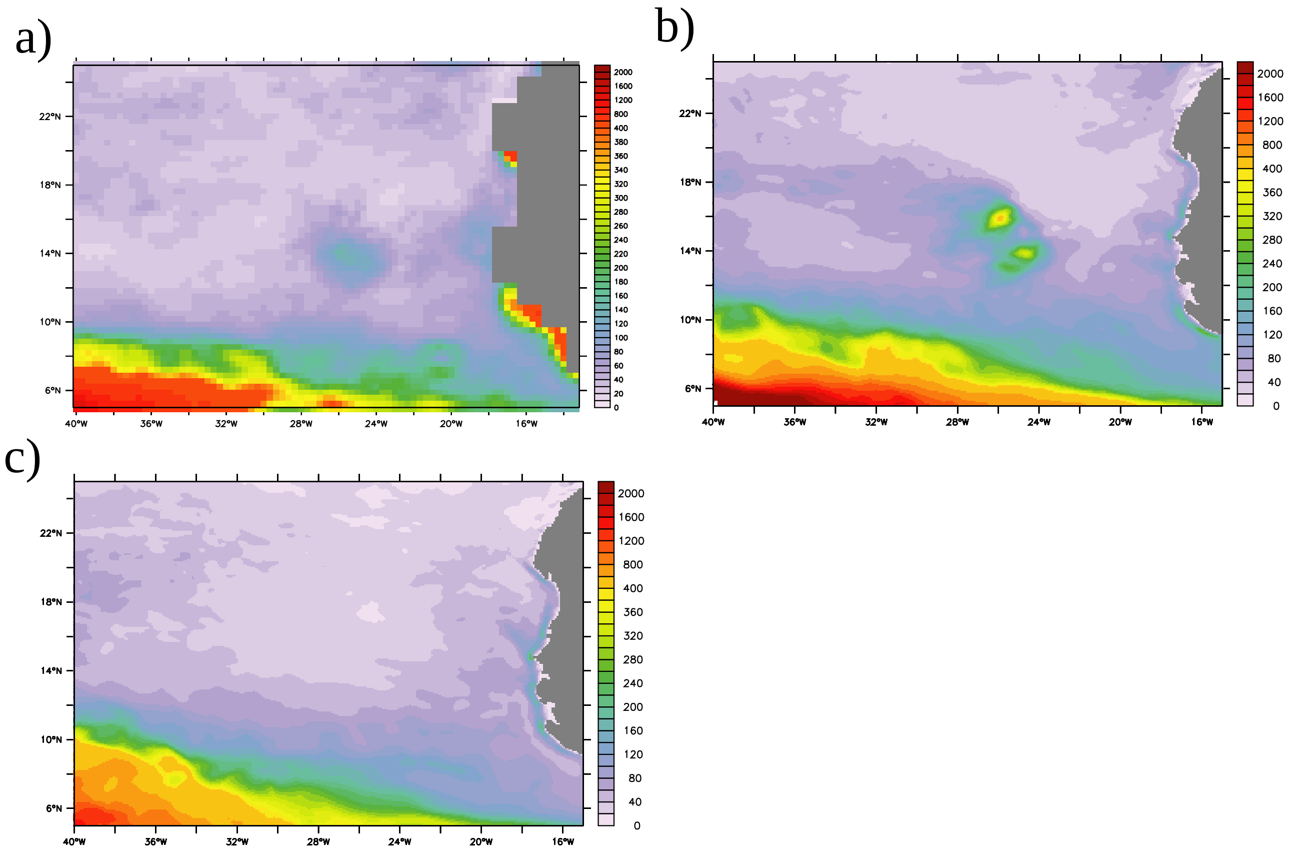

Figure 5: Eddy kinetic energy (EKE) derived from satellite altimeter observations of sea surface elevation data from AVISO in cm^2/s^2 (a) and from the OGCM with high-resolution forcing (exp. HIGH, b) and low-resolution forcing in wind stress (exp. LOW-WIND, c) in 20m depth calculated as velocity deviations from the average over 2001 to 2004 in cm^2/s^2.

by using the low resolution forcing during the spinup integration, the biomass- and chlorophyll-rich patch in lee of the Cape Verde Islands is not present anymore, but can be clearly identified in experiment HIGH. It can also be seen from Fig. 7 that near the Cape Verde Islands, chlorophyll is high in wintertime (January to April) consistent with strong wind speeds and high eddy activity in the same region in experiment HIGH as seen in Fig. 3.

Fig. 7 c) shows estimates of near surface chlorophyll from ocean color satellite observations taken from Sea-Wifs. The observations show a similar secondary maximum in the wake of the Cape Verde Islands as in the OGCM. Furthermore, this maximum shows up during wintertime both in experiment HIGH and in the observations. However, it is also clear that chlorophyll concentrations in SeaWifs are considerably higher compared to the model. One reason for this well-known discrepancy of the model with observations are certainly given by biases in the biogeochemical model. Among these biases are a wrong factor for conversion between nitrate content of phytoplankton and chlorophyll (which is not a prognostic variable of the model by itself), too fast phytoplankton depletion and too low recycling of nutrients in the mixed layer in the ecosystem model. On the other hand, it is also known that ocean color observations are especially in this region contaminated by sediment and Gelbstoff transport off the coastal upwelling regions and, in addition, by Sahara dust. However, it is evident in the figures that a secondary maximum in chlorophyll shows up near the Cape Verdes in both the model with high-resolution forcing and Seawifs, while this maximum is missing in the model with low-resolution forcing. Note that this result is further confirmed by direct observations of eddy-induced chlorophyll maxima near similar subtropical islands like the Canary Islands (Aristegui et al., 1997) or Hawaii (Seki et al.,

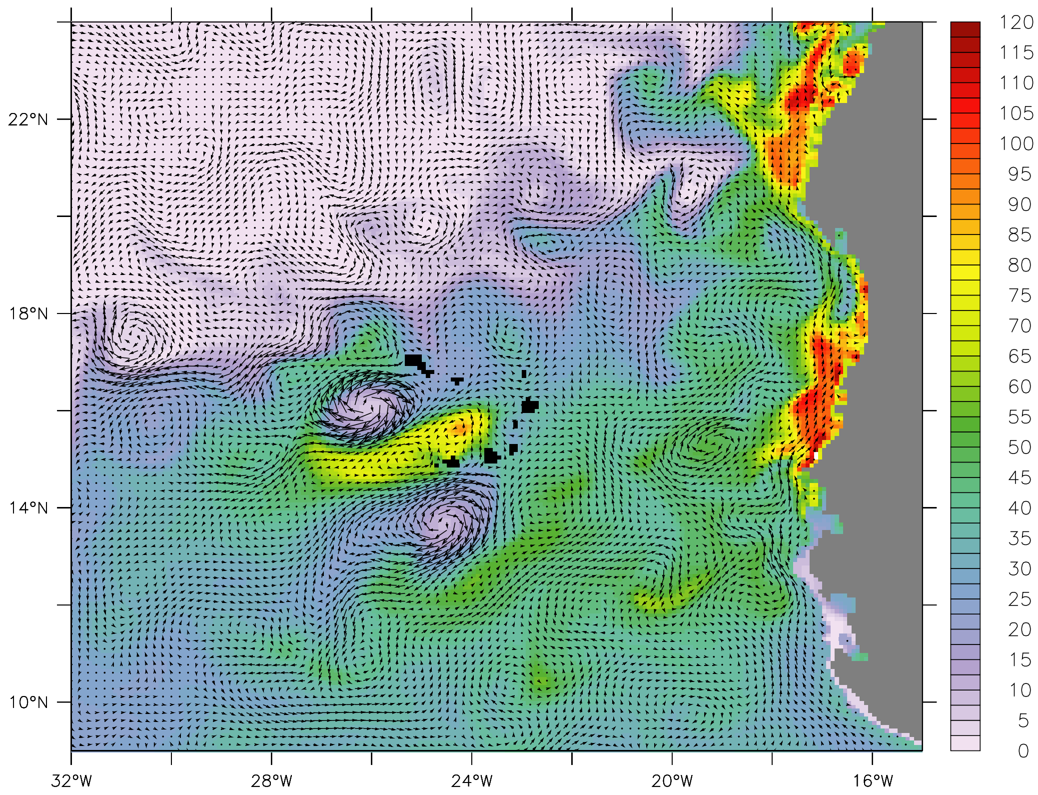

Figure 6: Biomass near Cape Verde on 20 February 2001 in the model integrated over the uppermost 100 m in mmol N/m^2. Also shown are the near surface velocities (arrows).

2001).

6 Summary and discussion

Using surface forcing from 2001 to 2004 taken from the operational high-resolution weather forecast model of the ECMWF to drive a high-resolution OGCM, we are able to demonstrate the impact of persistent small-scale features in near surface winds on cyclogenesis in the ocean. We have shown that such orographically forced small-scale features are present both in the latest ECMWF model version and in observational estimates of recent high-resolution satellite missions (Liu et al., 2000; Xie et al., 2001; Chelton et al., 2004). In our simulation, meso-scale oceanic eddies develop in the lee of Islands located in areas of prevailing trade winds such as the Cape Verde Islands. We are able to show that the high-resolution wind stress forcing is responsible for this cylogenesis, since such eddies are missing in simulations driven by low-resolution wind forcing and since they are still present driving the model with high-resolution wind stress forcing only. We note that these eddies can provide a substantial, previously overlooked source of oceanic eddy kinetic energy in subtropical regions. Furthermore, anticlockwise circulating eddies are related to upwelling of nutrient rich water from below leading to large plankton blooms in the simulations. EKE and near surface chlorophyll is in better agreement with observational estimates using the high-resolution forcing.

Note that similar eddies and related plankton blooms might also show up at comparable other locations in the world oceans, e.g. the Hawaiian Archipelago, with far-reaching implications for local and basin-wide ecosystem dynamics. Our results suggest that making full use of the potential of high-resolution coupled

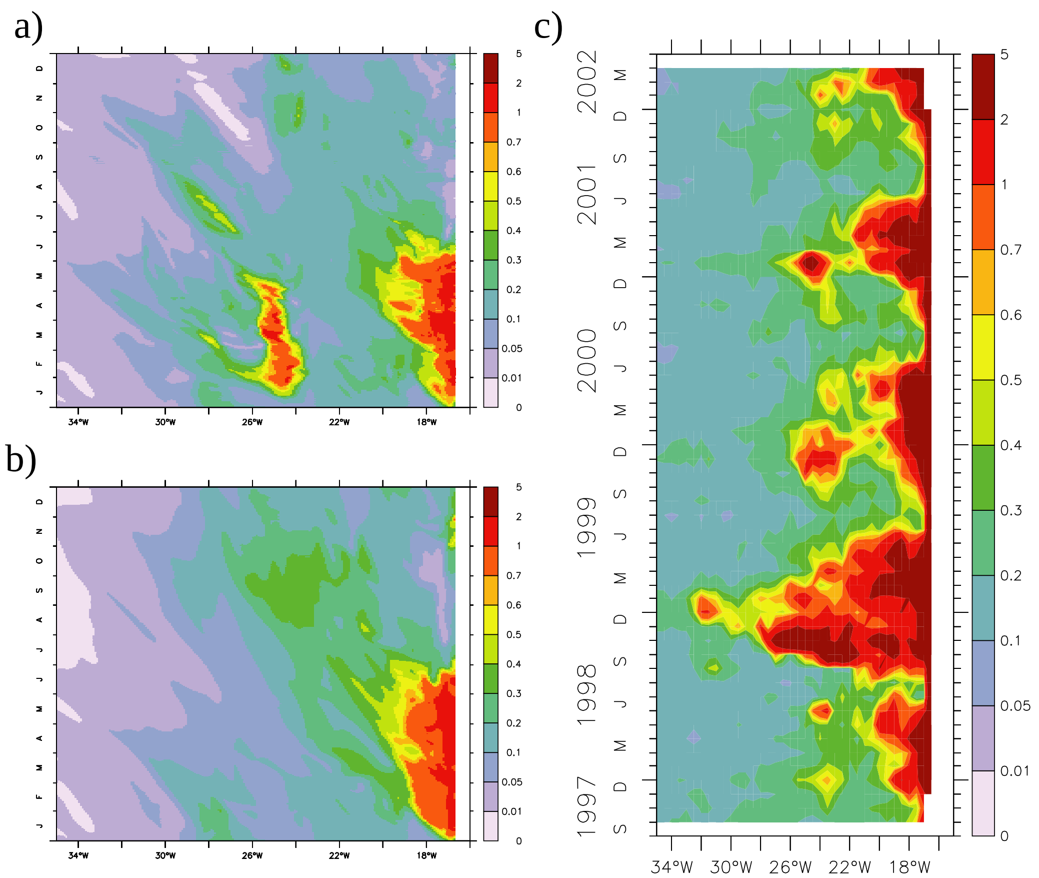

Figure 7: Near surface chlorophyll in mgChl/m^3 at a section along 15.5^{o}N in the model with high-resolution forcing (a), with climatological low-resolution forcing (b) and satellite observations (SeaWifs). We have used a factor of 1.59 mg/mmol to convert the nitrate content of phytoplankton averaged over the top 40 m in mmol N/m^3 to an equivalent chlorophyll concentration in mgChl/m^3.

ocean-ecosystem models by using high-resolution forcing fields from state-of-the-art NWP models might substantially improve our knowledge of the basin-wide effects of meso-scale variability on the ocean circulation and ecosystem.

Finally, we speculate that such eddy-enhanced plankton growth due to small-scale wind stress features in the subtropical oceans may contribute to explain the following, well-known inconsistency: Indirect geochemical estimates of nutrient supply to (Jenkins, 1988) and export of photosynthetically fixed material from the surface ocean (Jenkins, 1982) in the subtropical ocean are significantly higher than direct physical and biological observational estimates and model results suggest (Lewis et al., 1986; Oschlies and Garçon, 1998). A possible explanation are eddy-induced nutrient injections into the surface layer which might have been underestimated in observations and coarse resolution model studies (Jenkins, 1988; McGillicuddy and Robinson, 1997). Recent eddy-resolving model studies (Oschlies and Garçon, 1998; McGillicuddy and Robinson, 1997), however, suggest that open-ocean eddies are not sufficient to explain the gap. We speculate that atmospherically driven eddies in the lee of subtropical islands, which are missing in the previous model studies, might help to resolve this inconsistency.

Acknowledgments

The authors benefitted from discussions with Andrew Orr, Andreas Oschlies and Peter Rhines. This work was supported by the European Union within the projects NOCES and DYNAMITE.

References

Aristegui, J., P. Tett, A. Hernandez-Guerra, G. Basterretxea, M. F. Montero, K. Wild, P. Sangra, S. Hernandez-Leon, M. Canton, J. A. Garcia-Braun, M. Pacheco, and E. D. Barton, 1997: The influence of island-generated eddies on chlorophyll distribution: a study of mesoscale variation around Gran Canaria. *Deep-Sea Res.*, **44**(1), 71–96.

Barnier, B., L. Siefridt, and P. Marchesiello, 1995: Thermal forcing for a global ocean circulation model using a three year climatology of ECMWF analysis. *J. Mar. Sys.*, **6**, 363–380.

Chelton, D. B., M. G. Schlax, M. H. Freilich, and R. F. Milliff, 2004: Satellite measurements reveal persistent small-scale features in ocean winds. *Science*, **303**, 978–983.

Dengler, M., F. A. Schott, C. Eden, P. Brandt, J. Fischer, and R. J. Zantopp, 2004: Break-up of the Atlantic deep western boundary current into eddies at 8^oS. *Nature*, **432**, 1018–1020.

Eden, C. and T. Jung, 2001: North Atlantic interdecadal variability: oceanic response to the North Atlantic oscillation (1865–1997). *J. Climate*, **14**(5), 676–691.

Eden, C. and C. Oschlies, 2006: Adiabatic reduction of circulation-related CO_2 air-sea flux biases in North Atlantic carbon-cycle models. *Glob. Biochem. Cycles*. In press.

Frankignoul, C. and P. Müller, 1979: Quasigeostrophic response of an infinite beta-plane ocean to stochastic forcing by the atmosphere. *J. Phys. Oceanogr.*, **9**, 104–127.

Fratantoni, D. M., 2001: North Atlantic surface circulation during the 1990's observed with satellite-tracked drifters. *J. Geophys. Res.*, **106**, 22067–22093.

Gaspar, P., Y. Gregoris, and J.-M. Lefevre, 1990: A simple eddy kinetic energy model for simulations of the oceanic vertical mixing: tests at station PAPA and Long-Term Upper Ocean Study site. *J. Geophys. Res.*, **95**, 16179–16193.

Gill, A. E., 1982: *Atmosphere-ocean dynamics*. Academic Press, San Diego, CA.

Janssen, P., 2004: *The Interaction of Ocean Waves and Wind*. Cambridge University Press.

Jenkins, W. J., 1982: Oxygen untilization rates in the North Atlantic subtropical gyre and primary production in oligotrophic systems. *Nature*, **300**, 246–248.

Jenkins, W. J., 1988: Nitrate fluxes into the euphotic zone near Bermuda. *Nature*, **331**, 521–523.

Kalnay, E., M. Kanamitsu, R. Kistler, W. Collins, D. Deaven, L. Gandin, M. Iredell, S. Saha, G. White, J. Woollen, Y. Zhu, M. Chelliah, W. Ebiszusaki, W. Higgins, J. Janowiak, K. Mo, C. Ropelewski, J. Wang, A. Leetmaa, R. Reynolds, R. Jenne, and D. Joseph, 1996: The NCEP/NCAR 40-years reanalysis project. *Bull. Amer. Meteor. Soc.*, **77**, 437–471.

Le Traon, P. Y., P. Gaspar, F. Bouyssel, and H. Makhmara, 1995: Using TOPEX/POSEIDON data to enhance ERS-1 data. *J. Atm. Ocean. Techn.*, **12**, 161–170.

Lewis, M. R., W. G. Harrison, N. S. Oakey, D. Herbert, and T. Platt, 1986: Vertical nitrate fluxes in the oligotrophic ocean. *Science*, **234**, 870–873.

Liu, W. T., X. Xie, P. S. Polito, S. P. Xie, and H. Hashizume, 2000: Atmospheric manifestation of tropical instablity wave observed by QuikSCAT and tropical rain measuring mission. *Geophys. Res. Letters*, **27**(16), 2545–2548.

Mahfouf, J.-F. and F. Rabier, 2000: The ECMWF operational implementation of four-dimensional variational assimilation. II: Experimental results with improved physics. *Quart. J. Royal Met. Soc.*, **126**, 1171–1190.

McGillicuddy, D. J. J. and A. R. Robinson, 1997: Eddy-induced nutrient supply and new production in the Sargasso Ssea. *Deep-Sea Res.*, **44**, 1427–1450.

Müller, P. and C. Frankignoul, 1981: Direct atmospheric forcing of geostrophic eddies. *J. Phys. Oceanogr.*, **11**, 287–308.

Oschlies, A. and V. Garçon, 1998: Eddy induced enhancement of primary production in a model of the North Atlantic Ocean. *Nature*, **394**, 266–269.

Pacanowski, R. C., 1995: MOM 2 Documentation, User's Guide and Reference Manual. Technical report, GFDL Ocean Group, GFDL, Princeton, USA.

Rabier, F., H. Järvinen, E. Klinker, J.-F. Mahfouf, and A. Simmons, 2000: The ECMWF operational implementation of four-dimensional variational assimilation. I: Experimental results with simplified physics. *Quart. J. Royal Met. Soc.*, **126**, 1143–1170.

Schaer, C. and D. R. Durran, 1997: Vortex formation and vortex shedding in continuously stratified flows past isolated topography. *J. Atmos. Sci.*, **54**, 534–554.

Schott, F. and J. P. J. McCreary, 2001: The monsoon circulation of the Indian Ocean. *J. Geophys. Res.*, **51**, 1–123.

Seki, M. P., J. J. Polovina, R. E. Brainard, R. R. Bidigare, C. L. Leonard, and D. G. Foley, 2001: Biological enhancement at cyclonic eddies tracked with GOES thermal imagery in Hawaiian waters. *Geophys. Res. Letters*, **28**(8), 1583–1586.

Stammer, D. and C. W. Böning, 1996: *The Warmwatersphere of the North Atlantic Ocean*, chapter Generation and distribution of mesoscale eddies in the North Atlantic Ocean. Gebrüder Bornträger, Berlin, Germany.

Stammer, D., C. W. Böning, and C. Dieterich, 2001: The role of variable wind forcing in generating eddy energy in the North Atlantic. *Prog. Oceanogr.*, **48**(2–3), 289–312.

Uppala, S., P. W. Kallberg, A. J. Simmons, U. Andrae, V. Da Costa Bechtold, M. Fiorino, J. K. Gibson, J. Haseler, A. Hernandez, G. A. Kelly, X. Li, K. Onogi, S. Saarinen, N. Sokka, R. P. Allan, E. Andersson, K. Arpe, M. A. Balmaseda, A. C. M. Beljaars, L. van de Berg, J. Bidlot, N. Bormann, S. Caires, F. Chevallier, A. Dethof, M. Dragosavac, M. Fisher, M. Fuentes, S. Hagemann, E. Holm, B. J. Hoskins, L. Isaksen, P. A. E. M. Janssen, R. Jenne, A. P. McNally, J.-F. Mahfouf, J.-J. Morcrette, N. A. Rayner, R. W. Saunders, P. Simon, A. Sterl, K. E. Trenberth, A. Untch, D. Vasiljevic, P. Viterbo, and J. Woollen, 2006: The ERA-40 reanalysis. *Quart. J. Royal Met. Soc.*, **131**, 2961–3012.

Willebrand, J., B. Barnier, C. Böning, C. Dieterich, P. Killworth, C. LeProvost, Y. Jia, J. M. Molines, and A. L. New, 2001: Circulation characteristics in three eddy-permitting models of the North Atlantic. *Prog. Oceanogr.*, **48**(2–3), 123–161.

Wunsch, C. and R. Ferrari, 2004: Vertical mixing, energy and the general circulation of the oceans. *Annu. Rev. Fluid Mech*, **36**, 281–314.

Xie, S. P., W. T. Liu, Q. Liu, and M. Nonaka, 2001: Far-reaching effects of the Hawaiian Islands on the Pacific Ocean-Atmosphere system. *Science*, **292**, 2057–2060.